EASR

Engineering and Applied Science Research

https://www.tci-thaijo.org/index.php/easr/index

Published by the Faculty of Engineering, Khon Kaen University, Thailand

# Corrosion behavior of Sn-0.7Cu-xIn solders on simulated acid rain

Thammaporn Thublaor[1)], Thiraphong Nuanin[1)], Yoshiharu Mutoh[2)] and Kittichai Fakpan*[1)]

[1)]Department of Materials and Production Technology Engineering, Faculty of Engineering, King Mongkut's University of Technology North Bangkok, Bangkok 10800, Thailand
[2)]Nagaoka University of Technology, Nagaoka, Niigata 940-2188, Japan

Received 23 June 2025
Revised 17 September 2025
Accepted 14 October 2025

**Abstract**

This study investigated the effect of minor indium additions (0.1, 0.5, 1.0 wt.%) on Sn-0.7Cu solder, resulting in Sn-0.7Cu-0.1In, Sn-0.7Cu-0.5In, and Sn-0.7Cu-1.0In solders. The influence of indium addition on microstructure, melting temperature, microhardness, and corrosion resistance of the alloys was investigated. Corrosion resistance was evaluated in simulated acid rain with a pH of 3.5 using immersion and potentiodynamic polarization tests. Results indicated that the melting temperature decreased from 225.9 °C to 223.1 °C with increasing indium content. The addition of indium also refined the microstructure, reduced the β-Sn phase fraction, and improved the microhardness of the solder. Analysis of corrosion products identified SnO and $SnO_2$, confirming that tin is the primary element susceptible to corrosion in Sn-0.7Cu-xIn solders exposed to acidic conditions. Polarization curves revealed that corrosion resistance improved significantly with increasing indium content, with the lowest corrosion rate observed at 1.0 wt.% of indium.

**Keywords:** Sn-0.7Cu solder, Indium addition, Corrosion, Simulated acid rain

## 1. Introduction

Research on electronic materials has increasingly focused on the significant challenge of developing lead-free solders, an issue compounded by attempts to replace traditional Sn-Pb solders with the most effective lead-free alternatives [1-3]. Among these, ternary alloys such as Sn-Ag-Cu are promising lead-free replacements for conventional Sn-Pb solders [4-6]. Sn-0.7Cu solder, a widely used binary alloy, is particularly attractive due to its low cost and excellent overall performance [7]. However, it has notable disadvantages, including a relatively high melting temperature (227 °C) compared to Sn-37Pb solder (183 °C), limited oxidation resistance, and a shorter thermal cycling lifetime. Recently, research has focused on improving the mechanical and physical properties of Sn-0.7Cu solder through minor alloying additions. For instance, Yang et al. [8] reported that the addition of small amount of aluminum (0.010-0.075 wt.%) refines the microstructure and enhances the wettability of Sn-0.7Cu solder. The mechanical properties and wettability of tin-based lead-free solders can be enhanced by the addition of indium. El-Daly and Hammad [9] investigated the influence of silver and indium additions on the mechanical properties of Sn-0.7Cu solder. They found that these additions significantly increased the ultimate tensile strength and decreased the creep rate of the Sn-0.7Cu solder. Similarly, Nabihah and Nurulakmal [10] also reported that indium addition enhanced both the shear strength and wettability of Sn-0.7Cu solder. However, indium is expensive and scarce; thus, large-scale additions are not commercially viable [11]. Consequently, research has focused on small indium additions (lower than 1 wt.%), examining their effects on wettability, melting point, thermal expansion coefficient, hardness, and corrosion resistance [12, 13]. Li et al. [12] found that the addition of 0.3 wt.% indium decreased the corrosion rate of Sn-0.7Cu-0.2Ni alloy after two weeks of immersion in hydrochloric acid. Furthermore, the addition of indium should generally not exceed 1.0 wt.% since, in the Sn-1.0Ag-0.6Cu alloy, higher concentrations promote microstructural coarsening, which adversely affects mechanical properties [13].

Solder joint reliability is essential to the stability and performance of electronic packaging. Various factors can significantly affect solder reliability and dramatically reduce the lifetime of solder joints, including high temperatures, humidity, mechanical vibration, and corrosive environments [14]. Therefore, understanding the effect of extreme conditions on solder degradation is crucial in designing electronic packaging capable of withstanding them throughout its design lifetime. Corrosion resistance is especially important for solder alloys used in electronic devices exposed to aggressive operational environments. One of the primary causes of solder deterioration in outdoor electronic devices is corrosion caused by high humidity and rainwater, as these conditions can accelerate the corrosion processes [15]. In Asia, acid rain is a significant environmental issue, especially in industrialized regions. The formation of acid rain, which has a pH lower than 5.6, is primarily driven by significant atmospheric pollutants such as sulfur dioxide ($SO_2$) and nitrogen oxides ($NO_x$) [16]. Consequently, it is important to consider the effect of acid rain on solder corrosion. Few studies have investigated the corrosion behavior of lead-free solders under acidic conditions, with existing research primarily focused on hydrochloric acid solutions [17-19]. In contrast, Wierzbicka-Miernik et al. [20] investigated the corrosion behavior of Sn-Ag-Cu solders in a NaCl solution mixed with sulfuric and nitric acids (simulating acid rain). Despite this, little is known about how indium influences

*Corresponding author.
Email address: kittichai.f@eng.kmutnb.ac.th
https://doi.org/10.64960/easr.2026.262319

the corrosion resistance of Sn-0.7Cu solder under acidic conditions, specifically under simulated acid rain. Therefore, studying how indium affects the corrosion behavior of Sn-0.7Cu solder in simulated acid rain is essential for understanding the corrosion mechanisms and improving the longevity of solder joints used in outdoor electronic devices exposed to high-pollution environments. In this study, the corrosion resistance of Sn-0.7Cu solder with indium additions ranging from 0.1 to 1.0 wt.% was evaluated in simulated acid rain using immersion and potentiodynamic polarization tests. The resulting corrosion products were further characterized using scanning electron microscopy equipped with energy dispersive X-ray spectroscopy and X-ray diffraction to support the findings.

## 2. Materials and methodology

### *2.1 Solder alloys preparation and microstructure characterization*

In this study, four lead-free solders with compositions Sn-0.7Cu-xIn (x = 0, 0.1, 0.5, and 1.0 wt.%) were fabricated. The solder alloys were prepared from pure tin, copper, and indium (each with a purity greater than 99.9 wt.%), and melted in an alumina ($Al_2O_3$) crucible using an inductive furnace in an air at 600 °C for 60 min. A eutectic salt mixture of KCl and LiCl, in a weight ratio of 1.3:1.0, was used to cover the surface of the molten solder and prevent oxidation during the melting process. After melting, the molten solder was cooled down in a furnace to 300 °C and then cast into a steel mold to form a solder plate with dimensions of 100 ×100 × 10 $mm^3$. The chemical compositions of the as-cast solders were analyzed using an X-ray fluorescence spectrometer (XRF, HORIBA XGT-5200), as presented in Table 1. The as-cast solder plates were then cut into 10 ×10 × 10 $mm^3$ specimens for microstructural examination. The specimens were mechanically ground using SiC abrasive papers from 400 to 1200 grit and subsequently polished with a 0.03 µm $Al_2O_3$ suspension. The polished surfaces were then etched using a solution containing 2% HCl, 5% $HNO_3$, and 93% ethanol. Microstructural characterization was conducted using an optical microscope and scanning electron microscopy (SEM: FEI Quanta 450) equipped with energy dispersive X-ray spectroscopy (EDX). Phase identification was performed using X-ray diffraction (XRD: RIGAKU SmartLab) with CuKα radiation (λ = 1.5406 Å).

**Table 1** Chemical compositions of Sn-0.7Cu-xIn solders (wt.%)

| Solders | Sn | Cu | In |
|---|---|---|---|
| Sn-0.7Cu | 99.29 | 0.74 | - |
| Sn-0.7Cu-0.1In | 99.16 | 0.71 | 0.13 |
| Sn-0.7Cu-0.5In | 98.77 | 0.75 | 0.48 |
| Sn-0.7Cu-1.0In | 98.27 | 0.71 | 1.02 |

### *2.2 Thermal analysis*

The thermal behavior of Sn-0.7Cu-xIn solders was analyzed using differential scanning calorimetry (DSC: METTLER TOLEDO DSC 3+) under a nitrogen atmosphere. The temperature was increased from 25 °C to 300 °C at a constant heating rate of 5 °C/min. For each composition, three measurements were conducted using samples weighing approximately 0.03 g.

### *2.3 Mechanical testing*

The microhardness of Sn-0.7Cu-xIn solders was evaluated in accordance with of ASTM E92-17 [21] using a universal hardness tester (INNOVATEST Nemesis 5100G2). Three specimens of each composition were tested under a load of 1.961 N (200 gf) with a dwell time of 10 s. Fifteen indentations were made on each per specimen.

### *2.4 Corrosion testing*

The corrosion resistance of Sn-0.7Cu-xIn solders was investigated using immersion test in simulated acid rain at room temperature for up to 50 days, following ASTM G31-21 [22]. For each solder composition, three specimens dimensions of 10 ×10 × 10 $mm^3$ were cut from as-cast solder plates. All surfaces were mechanically ground with 1000 grit SiC abrasive paper prior to testing. During the immersion test, specimens were weighed every five days to record cumulative mass loss using a five-digit digital balance. Simulated acid rain was prepared by mixing 1 mol/$dm^3$ nitric acid ($HNO_3$) and 1 mol/$dm^3$ sulfuric acid ($H_2SO_4$) in a 1:2 molar ratio [23]. The mixture was then diluted with deionized water to obtain a final solution with a pH of 3.5. According to the Acid Deposition Monitoring Network in East Asia (EANET) [24], the annual mean pH of rainfall in Thailand is approximately 5, while in the industrialized regions, such as Chonburi and Rayong provinces, the lowest recorded pH values reached about 3.2. Based on these findings, a pH of 3.5 was selected for this study to simulate acid rain and represent a worst-case scenario for accelerated corrosion testing. For each test, 200 $cm^3$ of simulated acid rain was used, and the solution was renewed at five-day intervals. Before weighing, the specimens were cleaned with deionized water using an ultrasonic cleaning machine and dried in a stream of air. The corrosion rate was calculated using the following equation.

$$CR = \frac{KW}{ATD} \quad (1)$$

In this equation, *CR* denotes the corrosion rate in µm/year, *K* is a constant ($8.76 \times 10^7$), *T* is the exposure time in hours, *A* is the exposure surface area in $cm^2$, *W* is the cumulative mass loss after immersion for a maximum period of 50 days in g, and *D* is the density in g/$cm^3$. The density of Sn-0.7Cu solder was taken as 7.323 g/$cm^3$ [25].

Potentiodynamic polarization tests were also performed in simulated acid rain with a pH of 3.5. The tests were carried out using three-electrode cells consisting of a silver/silver chloride reference electrode, a platinum rod counter electrode, and a solder specimen working electrode. Prior to testing, the specimens were polished, rinsed with deionized water, and then dried. At least two experiments were conducted for each condition, at room temperature. Each specimen was initially equilibrated by monitoring the open-circuit

potential (OCP) for 30 min. Polarization measurements were subsequently carried out at a scan rate of 0.001 V/s within a potential range of −0.5 V to +0.7 V relative to the OCP.

## 3. Results and discussion

### *3.1 Melting temperature of the solders*

The melting temperature of solder alloys is a critical factor in determining their suitability for electronic packaging processes. Excessively high soldering temperature, required by high melting point solders, can lead to thermal damage and component failure. Figure 1 shows the differential scanning calorimetry (DSC) curves of Sn-0.7Cu-xIn solders. Each curve displays a single endothermic peak, with the peak temperature decreasing as the indium content increased. This result indicates that the melting temperatures of Sn-0.7Cu-xIn solders significantly decreased with increasing indium content. Specifically, the melting temperature of the solders decreased from 225.9 °C to 223.1 °C as the indium content increased from 0.1 to 1.0 wt.%.

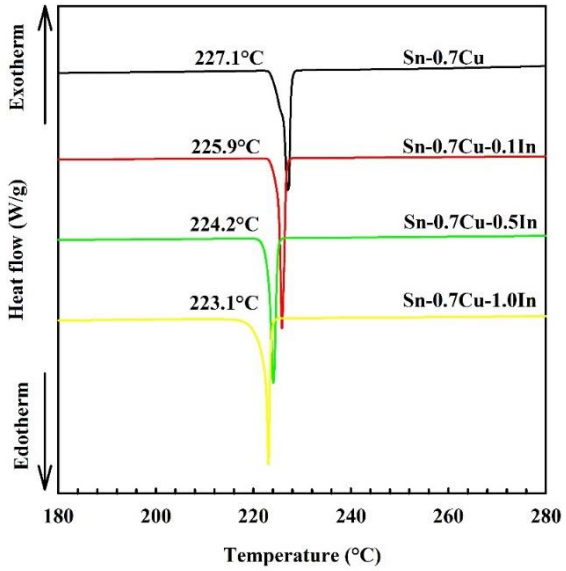


**Figure 1** Differential scanning calorimetry (DSC) curves of Sn-0.7Cu-xIn solders

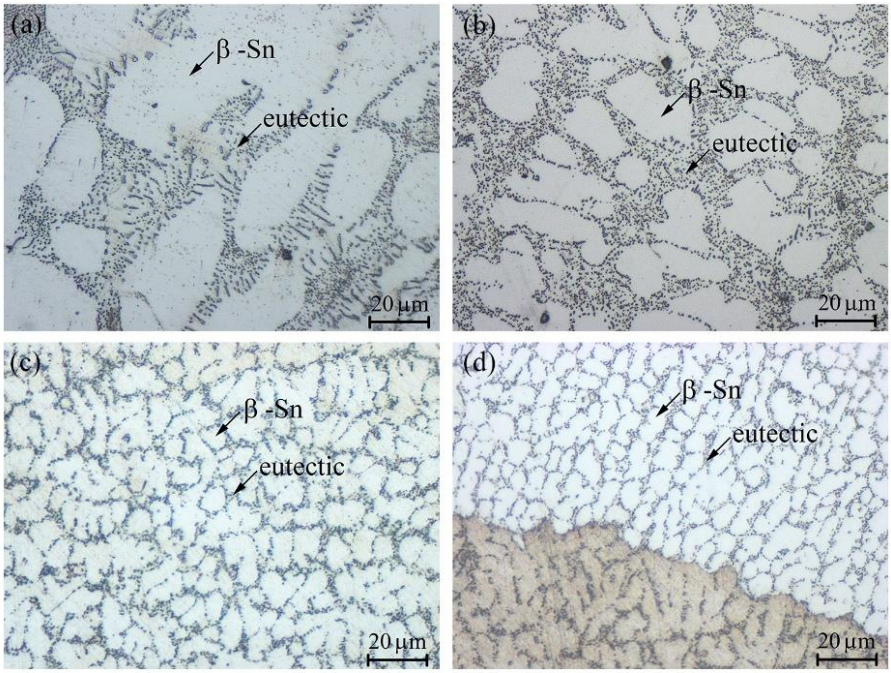


**Figure 2** Optical micrographs showing the microstructure of (a) Sn-0.7Cu, (b) Sn-0.7Cu-0.1In, (c) Sn-0.7Cu-0.5In, and (d) Sn-0.7Cu-1.0In solders

### *3.2 Microstructure and microhardness of solders*

The microstructure of the Sn-0.7Cu-xIn solders consisted of the β-Sn phase and eutectic phase of dispersed intermetallic compound (IMC), as depicted in Figure 2. As clearly observed in the figure, the β-Sn colonies in Sn-0.7Cu solder were significantly larger than

those in the Sn-0.7Cu-0.1In, Sn-0.7Cu-0.5In, and Sn-0.7Cu-1.0In solders. The results of the average β-Sn colony size, phase fraction (analyzed using NIKON NIS-Elements), and microhardness values are reported in Table 2. These results reveal that increasing indium content reduced both the average β-Sn colony size and β-Sn phase fraction. Previous studies [9, 26, 27] reported that the addition of indium to Sn-0.7Cu solder reduced the growth of large β-Sn dendritic structures while promoting the formation of the eutectic $Cu_6Sn_5$ phase within the β-Sn matrix. The effect is attributed to the presence of γ-$SnIn_4$ intermetallic compound. Indium addition refines the microstructure of Sn-0.7Cu solder by lowering the degree of supercooling, promoting heterogeneous nucleation, and accelerating nucleation during the solidification process [28]. The resulting finer microstructure enhances the microhardness of the solders, primarily through fine-grain strengthening.

**Table 2** Average β-Sn colony size and phase fraction of Sn-0.7Cu-xIn solders

| Solders | Microhardness (Hv) | Average β-Sn colony size (μm) | Phase fraction (%) | |
|---|---|---|---|---|
| | | | β-Sn | Eutectic |
| Sn-0.7Cu | 12.7 ± 0.6 | 59 ± 9 | 73 ± 3 | 27 ± 2 |
| Sn-0.7Cu-0.1In | 13.2± 0.4 | 29 ± 7 | 69 ± 3 | 31 ± 3 |
| Sn-0.7Cu-0.5In | 13.7± 0.7 | 18 ± 8 | 65 ± 4 | 35 ± 4 |
| Sn-0.7Cu-1.0In | 15.2± 0.6 | 16 ± 7 | 64 ± 2 | 36 ± 3 |

According to the equilibrium phase diagram of Sn-Cu-In, indium can dissolve in the β-Sn phase as a solid solution atom and form intermetallic compounds such as $Cu_6(Sn, In)_5$ and $Cu_3In$ through interaction with Sn and Cu [29]. Consequently, the addition of indium to Sn-Cu solder modifies the intermetallic compound, transforming $Cu_6Sn_5$ IMC into $Cu_6(Sn, In)_5$ IMC [30, 31]. Notably, the $Cu_6Sn_5$ and $Cu_6(Sn, In)_5$ IMCs have the same crystal structure [31]. XRD analysis was performed on all the as-cast Sn-0.7Cu-xIn solders, and the corresponding XRD patterns are shown in Figure 3. The patterns for all compositions confirmed the presence of body-centered tetragonal β-Sn (ICDD:03-065-7657) and $Cu_6Sn_5$ IMC (ICDD:01-076-2703) phases, indicating that tin and copper are main constituents involved in solidification. However, due to the structural similarity between $Cu_6Sn_5$ and $Cu_6(Sn, In)_5$ IMCs, these phases cannot be reliably distinguished by XRD analysis. Therefore, the presence of $Cu_6(Sn, In)_5$ IMC should be confirmed using a complementary characterization technique.

To confirm the formation of $Cu_6(Sn, In)_5$ IMC in Sn-0.7Cu-xIn solders, element analysis at intermetallic compound regions was further analyzed using EDX. SEM micrographs with corresponding analysis points and EDX spectra for the Sn-0.7Cu-xIn solders are shown in Figure 4. The atomic percentages of elements within the intermetallic compound, obtained from EDX spectra for the different solders, are summarized in Table 3. The addition of indium in the range of 0.1 to 1.0 wt.% led to an increase in the indium atomic percentage within the intermetallic compound from 0.26 to 0.39 at.%. Moreover, the atomic ratio of Cu to (Sn, In) remained approximately 6:5, confirming the formation of the $Cu_6(Sn, In)_5$ IMC in the Sn-0.7Cu solder with minor indium additions.

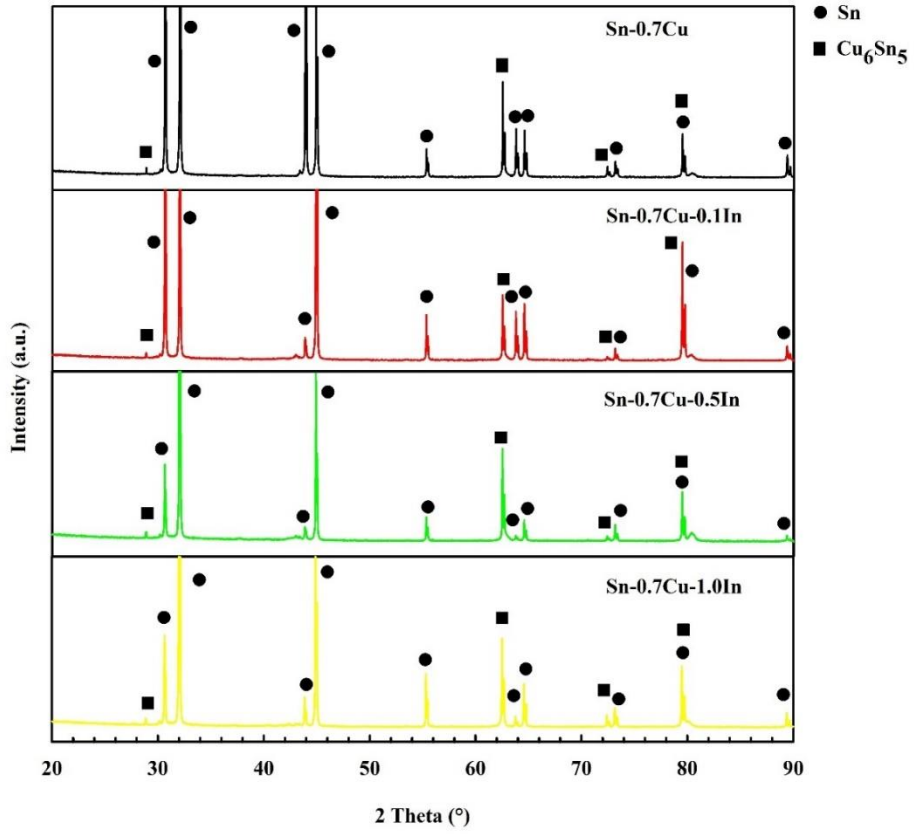


**Figure 3** X-ray diffraction (XRD) patterns of the as-cast Sn-0.7Cu-xIn solders

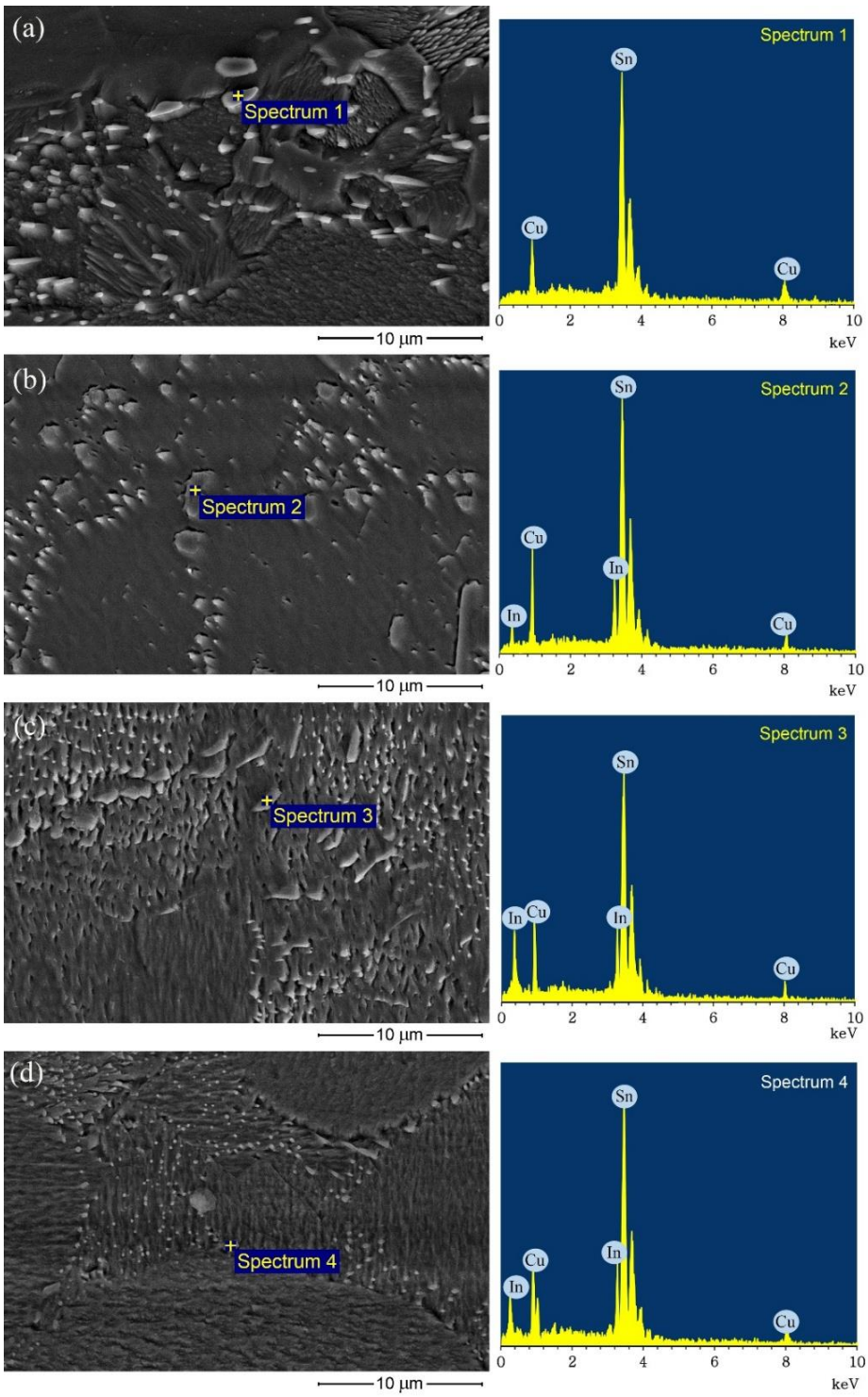


**Figure 4** SEM micrographs and corresponding EDX spectra of intermetallic compounds for (a) Sn-0.7Cu, (b) Sn-0.7Cu-0.1In, (c) Sn-0.7Cu-0.5In, and (d) Sn-0.7Cu-1.0In solders

**Table 3** Chemical composition (at.%) of intermetallic compounds and Cu:(Sn, In) atomic ratio for Sn-0.7Cu-xIn solders

| Solders | Cu (at.%) | Sn (at.%) | In (at.%) | Cu:(Sn, In) ratio |
|---|---|---|---|---|
| Sn-0.7Cu | 54.87 | 45.13 | ND | 6:4.93 |
| Sn-0.7Cu-0.1In | 54.42 | 45.32 | 0.26 | 6:5.02 |
| Sn-0.7Cu-0.5In | 54.11 | 45.58 | 0.31 | 6:5.08 |
| Sn-0.7Cu-1.0In | 54.32 | 45.29 | 0.39 | 6:5.04 |

*3.3 Corrosion resistance of Sn-0.7Cu-xIn solders*

Figure 5 shows the mass loss per unit area of Sn-0.7Cu-xIn solders after immersion in simulated acid rain with a pH of 3.5 for up to 50 days. The cumulative mass losses of Sn-0.7Cu, Sn-0.7Cu-0.1In, Sn-0.7Cu-0.5In, and Sn-0.7Cu-1.0In solders after immersion 50

days were 1.52, 1.27, 0.92 and 0.69 mg/cm$^2$, respectively. Among the solder compositions, Sn-0.7Cu-1.0In exhibited the lowest mass loss, which was significantly lower than those of the other solders. Table 4 summarizes the corrosion rates calculated using Equation (1), including their corresponding error bar ranges. The Sn-0.7Cu-1.0In solder showed the lowest corrosion rate, indicating its superior resistance to dissolution in simulated acid rain. Figure 6 shows SEM images of the surface morphology of Sn-0.7Cu-xIn solders after 50 days of immersion. Corrosion pits were observed across the surfaces of all the solders.

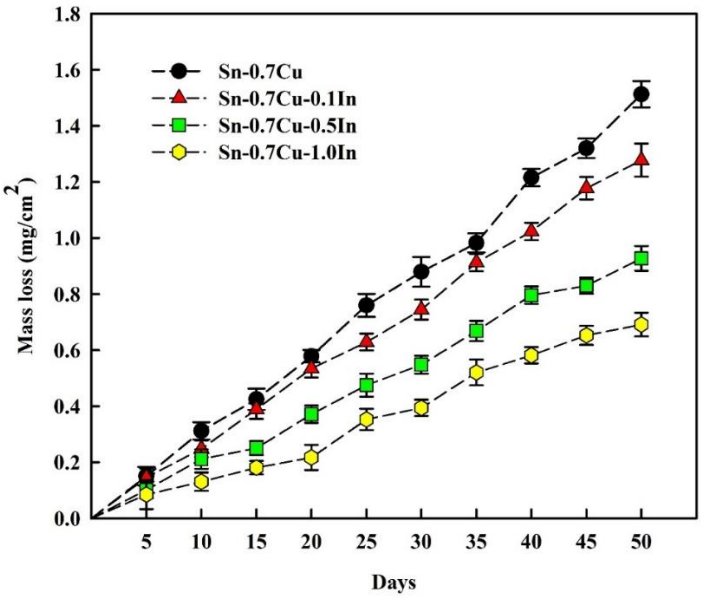


**Figure 5** Cumulative mass loss per unit area of Sn-0.7Cu-xIn solders as a function of immersion time in a simulated acid with a pH of 3.5

**Table 4** Corrosion rates of Sn-0.7Cu-xIn solders after 50 days of immersion in simulated acid rain with a pH of 3.5

| Solders | Corrosion rate (μm/year) |
|---|---|
| Sn-0.7Cu | 15.3 ± 0.7 |
| Sn-0.7Cu-0.1In | 12.7 ± 0.8 |
| Sn-0.7Cu-0.5In | 9.3 ± 0.8 |
| Sn-0.7Cu-1.0In | 6.9 ± 0.6 |

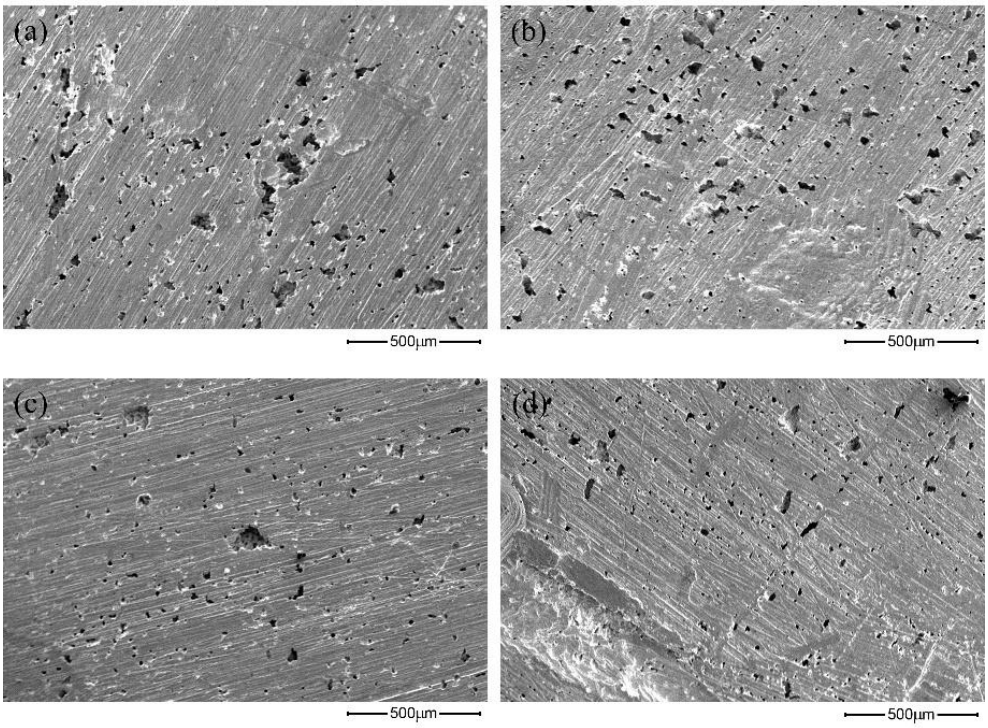


**Figure 6** SEM images showing the surface morphology of (a) Sn-0.7Cu, (b) Sn-0.7Cu-0.1In, (c) Sn-0.7Cu-0.5In, and Sn-0.7Cu-1.0In solders after 50 days of immersion in simulated acid with a pH of 3.5

The high magnification SEM images in Figure 7 show the corrosion product formed within the pits. The corresponding EDS spectra detected only tin and oxygen, with no copper and indium present. This indicated that the corrosion products are probably tin oxides, specifically SnO and $SnO_2$.

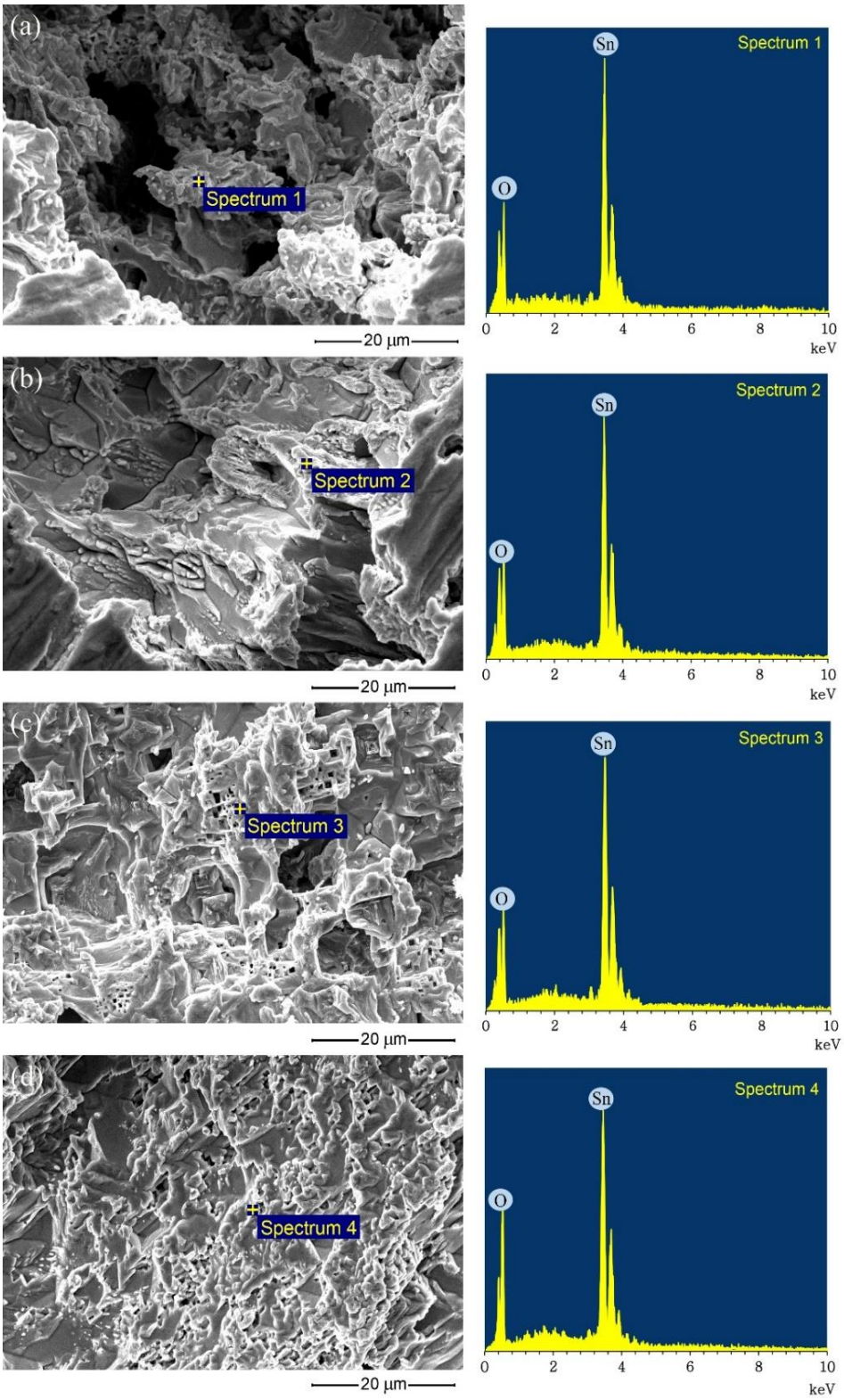


**Figure 7** SEM images and corresponding EDX spectra of corrosion pits on (a) Sn-0.7Cu, (b) Sn-0.7Cu-0.1In, (c) Sn-0.7Cu-0.5In, and (d) Sn-0.7Cu-1.0In solders after 50 days of immersion in simulated acid rain with a pH of 3.5

Figure 8 presents XRD patterns of Sn-0.7Cu-xIn solders after 50 days of immersion in simulated acid rain with a pH of 3.5. The detected phases include β-Sn phase (ICDD:03-065-7657), $Cu_6Sn_5$ (ICDD:01-076-2703), SnO (ICDD:01-077-2296), and $SnO_2$ (ICDD:00-029-1484). These results confirm that tin is the primary element susceptible to corrosion in simulated acid rain, leading to the formation of SnO and $SnO_2$.

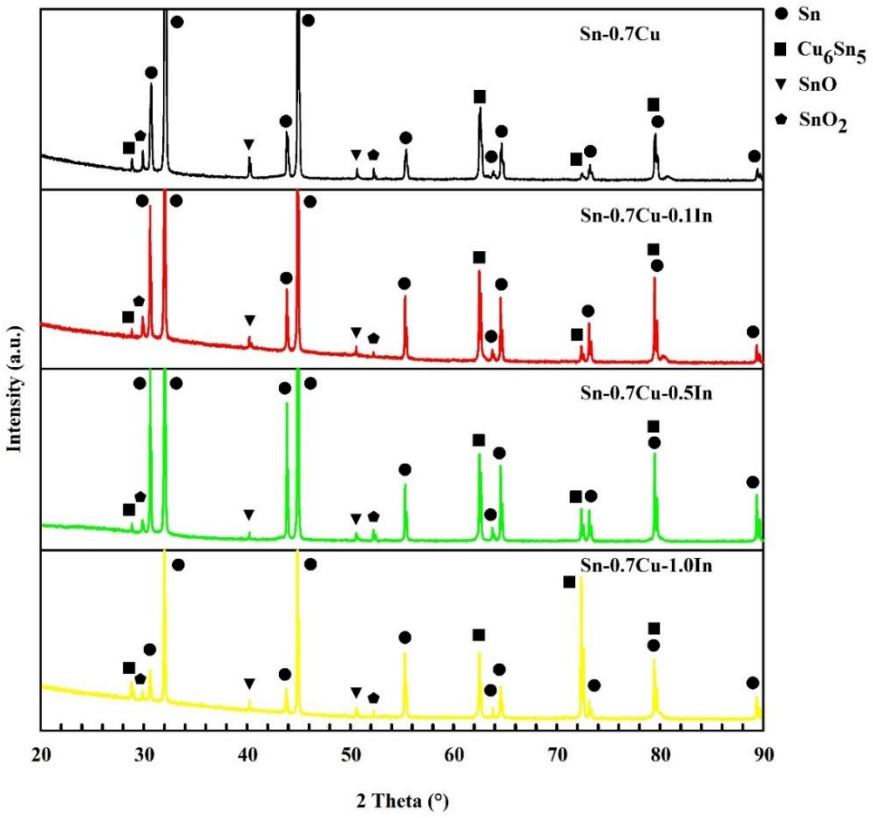


**Figure 8** XRD diffraction (XRD) patterns of Sn-0.7Cu-xIn solders after 50 days of immersion in simulated acid rain with a pH of 3.5

Figure 9 presents the polarization curves of Sn-0.7Cu-xIn solders tested in simulated acid rain with a pH of 3.5. All the solder samples exhibited a similar profile, characterized by a cathodic region (from point A to B) and an anodic active region (from point B to C). An enlarged portion of the polarization curves, also shown in Figure 9, allows for a clearer comparison of the corrosion potentials of the different Sn-0.7Cu-xIn solders. Using Tafel extrapolation principle, the electrochemical parameters of the solder were determined, and are summarized in Table 5.

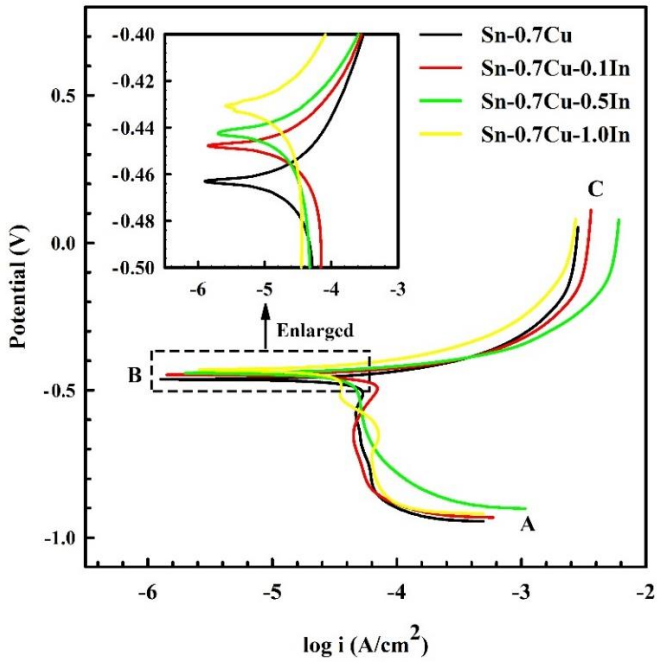


**Figure 9** Polarization curves of Sn-0.7Cu-xIn solders after immersion in simulated acid rain with a pH of 3.5

The corrosion potential ($E_{corr}$) of Sn-0.7Cu solder was measured at –0.462 V. With the addition of indium, $E_{corr}$ increased slightly, by approximately 6.7 %, reaching a maximum value of –0.431 V. Concurrently, the corrosion current density ($i_{corr}$) decreased with increasing indium content, showing a reduction of approximately 31.4% and reaching a minimum value of $1.12 \times 10^{-5}$ A/cm$^2$ at 1.0 wt.% indium. These findings suggest that increasing the indium content improves the corrosion resistance of Sn-0.7Cu solder by reducing its susceptibility to electrochemical degradation.

**Table 5** Polarization parameters of Sn-0.7Cu-xIn solders after immersion in simulated acid rain with a pH of 3.5

| Sample | $E_{corr}$ (V) | $i_{corr}$ (A/cm$^2$) |
|---|---|---|
| Sn-0.7Cu | –0.462 | $1.63 \times 10^{-5}$ |
| Sn-0.7Cu-0.1In | –0.448 | $1.26 \times 10^{-5}$ |
| Sn-0.7Cu-0.5In | –0.441 | $1.21 \times 10^{-5}$ |
| Sn-0.7Cu-1.0In | –0.431 | $1.12 \times 10^{-5}$ |

Most metal corrosion processes occur through electrochemical reactions at the interface between the metal surface and the surrounding electrolyte. These processes consist of two half-cell reactions: oxidation at the anodic region and reduction at the cathodic region. In the acidic solution such as simulated acid rain, the primary cathodic reaction is oxygen reduction reaction [32]. In the anodic region, the electrochemical reaction is driven by the dissolution of the metal from the alloy surface. Both $HNO_3$ and $H_2SO_4$ in the solution act as strong oxidizing agents capable of rapidly attacking metals. For Sn-Cu solders, numerous studies have reported the preferential dissolution of tin in NaCl solution [33-37]. Similarly, in acidic environments, tin is the primary element that dissolves [38-41], consistent with the findings of this work.

Figure 9 shows that the corrosion potentials of Sn-0.7Cu-xIn solders were approximately –0.4 V, which can be attributed to the preferential dissolution of tin. Although indium is the most electrochemically active element in the Sn-0.7Cu-xIn solders, as indicated by its dissolution potential [42], its relatively low content results in rapid leaching during corrosion. Consequently, tin becomes the next most electrochemically active species. Tin has a standard electrode potential lower than that of copper, as well as $Cu_3Sn$ and $Cu_6Sn_5$ intermetallic compounds [40, 43, 44], increasing its susceptibility to dissolution under corrosive conditions. Therefore, tin is considered the primary element undergoing dissolution in Sn-0.7Cu-xIn solders. The dissolution reaction of solder in acidic solution can be described as follows [38, 40, 41]:

$$Sn_{(s)} + \frac{1}{2}O_2 + 2H^+_{(aq)} \rightarrow Sn^{2+}_{(aq)} + H_2O \quad (2)$$

In aerated solutions, tin ions react with dissolved oxygen to form intermediate tin hydroxide species ($Sn(OH)_x$), as described by Reactions (3) and (4) [34-40]:

$$Sn^{2+}_{(aq)} + 2H_2O \rightarrow Sn(OH)_2 + 2H^+_{(aq)} \quad (3)$$

$$2Sn^{2+}_{(aq)} + O_2 + 6H_2O_{(aq)} \rightarrow 2Sn(OH)_4 + 4H^+_{(aq)} \quad (4)$$

These intermediates subsequently dehydrate, leading to the formation of tin oxide, as shown in Reactions (5) and (6) [34-40]:

$$Sn(OH)_2 \rightarrow SnO_{(s)} + H_2O \quad (5)$$

$$Sn(OH)_4 \rightarrow SnO_{2(s)} + 2H_2O \quad (6)$$

According to the XRD analysis, both SnO and $SnO_2$ were detected on the Sn-0.7Cu-xIn solders, while no copper oxides were observed, indicating that tin oxides were the primary corrosion products. Although $HNO_3$ is a strong oxidizing agent capable of directly dissolve copper, it does not promote the formation of a protective oxide film on the copper surface [32, 41]. The Pourbaix diagram of the copper-water system further indicates that copper corrodes by releasing copper ions in solutions with pH values below 5. Thus, in the simulated acid rain with a pH of 3.5, copper undergoes corrosion without forming a stable oxide film [32, 45].

The addition of indium to Sn-Cu solder influences its corrosion resistance, through changes in chemical composition and microstructure. In this study, the addition of indium to Sn-0.7Cu solder reduced the average β-Sn colony size from 59 μm (Sn-0.7Cu) to 16 μm (Sn-0.7Cu-1.0In). Additionally, the β-Sn phase fraction decreased from 73% to 64% with 1 wt.% indium addition. Thus, the addition of indium to Sn-Cu solder reduced the β-Sn phase fraction, increased the eutectic fraction, and resulted in overall microstructural refinement. Previous studies [9, 26, 27] reported that β-Sn phase partial refinement, resulted in the formation of a fine and uniform distribution of $Cu_6Sn_5$ and γ-$InSn_4$ intermetallic compounds within the eutectic zones of the solidified microstructure. This effect is attributed to the effective role of indium in generating nucleation sites during solidification in Sn-0.7Cu solder [28]. Similarly, the addition of indium has been shown to promote the refinement of the Sn-rich phase and a uniform distribution of the intermetallic compounds in Sn-0.3Ag-0.7Cu solder [46]. Jaiswal et al. [35] investigated the influence of indium addition on the corrosion behavior of Sn-Cu solder. They reported that indium addition promoted a uniform microstructure and refinement of β-Sn grains. Furthermore, increasing indium content in Sn-Cu solder resulted in a lower corrosion current density and a higher corrosion potential. The addition of indium to Sn-2Cu solder reduced the size of large intermetallic compounds and refined the microstructure by producing smaller β-Sn grains, thereby enhancing corrosion resistance due to reduced size of the intermetallic phase [28]. The potential difference between the β-Sn phase and the eutectic phase, which contains dispersed intermetallic compounds, results in the eutectic phase acting as the cathodic region, as the $Cu_6Sn_5$ IMC is electrochemically nobler than the β-Sn phase [35, 44]. Consequently, the eutectic phase fraction served as the cathodic region for oxygen reduction, which was coupled with the oxidation of tin in the β-Sn phase. The reduction in the β-Sn phase fraction consequently decreased the rate of tin dissolution, as evidenced by the lowest corrosion current density observed for Sn-0.7Cu-1.0In. It can be concluded that the addition of indium enhanced the corrosion resistance of Sn-0.7Cu-xIn solders by reducing the β-Sn phase fraction and limiting tin dissolution in the β-Sn phase. Therefore, the refined microstructure is a key factor contributing to the enhanced corrosion resistance observed in Sn-Cu solders [35, 36]. Overall, this study demonstrated that adding 0.1-1.0 wt.% indium enhanced the corrosion resistance of the Sn-0.7Cu solders through refining the β-Sn phase fraction and the formation of smaller, more uniformly distributed intermetallic compounds.

## 4. Conclusions

The corrosion resistance of Sn-0.7Cu-xIn solders with x = 0.1, 0.5, and 1.0 wt.% was investigated through immersion and potentiodynamic polarization tests in simulated acid rain with a pH of 3.5. The main findings are summarized as follows:

Increasing the indium content from 0.1 to 1.0 wt.% decreased the melting temperature of Sn-0.7Cu solder from 225.9 °C to 223.1 °C. The microstructure of Sn-0.7Cu solder consists of β-Sn and a eutectic phase containing dispersed $Cu_6Sn_5$ intermetallic compounds. Indium addition reduced the β-Sn phase fraction, increased the eutectic fraction, and refined the overall microstructure in Sn-0.7Cu-0.1In, Sn-0.7Cu-0.5In, and Sn-0.7Cu-1.0In solders. Immersion tests revealed that the addition of 0.1 to 1.0 wt.% indium significantly reduced the corrosion rate of Sn-0.7Cu solder. Analysis of corrosion products confirmed the formation of SnO and $SnO_2$, indicating tin as the primary element undergoing corrosion in Sn-0.7Cu-xIn solders exposed to simulated acid rain.

Polarization measurements further revealed that corrosion resistance improved with increasing indium content, as evidenced by a decrease in corrosion current density ($i_{corr}$), and an increase in corrosion potential ($E_{corr}$). This enhancement is attributed to indium-induced microstructural refinement, specifically the reduction in β-Sn colony size and the formation of smaller, more uniformly distributed intermetallic compounds.

## 5. Acknowledgement

This research budget was allocated by National Science, Research and Innovation Fund (NSRF) and King Mongkut's University of Technology North Bangkok (KMUTNB-FF-68-A-08)

## 6. Author contribution

Thammaporn Thublaor: Conceptualisation, Methodology, Data curation, Validation, Visualisation, Writing-original draft, Writing-review and editing, Resources, Funding acquisition, Project administration, Supervision; Thiraphong Nuanin: Methodology; Yoshiharu Mutoh: Supervision; Kittichai Fakpan: Conceptualisation, Methodology, Investigation, Formal Analysis, Data curation, Validation, Visualisation, Writing-original draft, Writing-review and editing, Resources, Funding acquisition, Project administration, Supervision

## 7. References

[1] Cheng S, Huang CM, Pecht M. A review of lead-free solders for electronics applications. Microelectron Reliab. 2017;75:77-95.
[2] Mallampati S, Yin L, Shaddock D, Schoeller H, Cho J. Lead-free alternatives for interconnects in high-temperature electronics. J Electron Packag. 2018;140(1):010906.
[3] Jiang N, Zhang L, Liu ZQ, Sun L, Long WM, He P, et al. Reliability issues of lead-free solder joints in electronic devices. Sci Technol Adv Mater. 2019;20(1):876-901.
[4] Fahim A, Ahmed S, Suhling JC, Lall P. Mechanical characterization of intermetallic compounds in SAC solder joints at elevated temperatures. 2018 17th IEEE Intersociety Conference on Thermal and Thermomechanical Phenomena in Electronic Systems (ITherm); 2018 May 29 - Jun 1; San Diego, USA. USA: IEEE; 2018. p. 1081-90.
[5] Ahmed S, Hasnine M, Suhling JC, Lall P. Mechanical characterization of SAC solder joints at high temperature using nanoindentation. 2017 IEEE 67th Electronic Components and Technology Conference (ECTC); 2017 May 30 - Jun 2; Orlando, USA. USA: IEEE; 2017. p. 1128-35.
[6] Akkara FJ, Hamasha S, Alahmer A, Evans J, Belhadi MEA, Wei X. The effect of micro-alloying and surface finishes on the thermal cycling reliability of doped SAC solder alloys. Materials. 2022;15(19):6759.
[7] Salleh MAAM, Al Bakri AMM, Somidin F, Sandu AV, Saud N, Kamaruddin H, et al. A comparative study of solder properties of Sn–0.7Cu lead-free solder fabricated via the powder metallurgy and casting methods. Revista de Chimie. 2013;64(7):725-8.
[8] Yang L, Zhang Y, Dai J, Jing Y, Ge J, Zhang N. Microstructure, interfacial IMC and mechanical properties of Sn–0.7Cu–xAl (x= 0–0.075) lead-free solder alloy. Mater Des. 2015;67:209-16.
[9] El-Daly AA, Hammad AE. Development of high strength Sn–0.7Cu solders with the addition of small amount of Ag and In. J Alloys Compd. 2011;509(34):8554-60.
[10] Nabihah A, Nurulakmal MS. Effect of In addition on microstructure, wettability and strength of SnCu solder. Mater Today: Proc. 2019;17:803-9.
[11] Fazal MA, Liyana NK, Rubaiee S, Anas A. A critical review on performance, microstructure and corrosion resistance of Pb-free solders. Measurement. 2019;134:897-907.
[12] Li LF, Cheng YK, Xu GL, Wang EZ, Zhang ZH, Wang H. Effects of indium addition on properties and wettability of Sn–0.7 Cu–0.2 Ni lead-free solders. Mater Des. 2014;64:15-20.
[13] Wang J, Yin M, Lai Z, Li X. Wettability and microstructure of Sn-Ag-Cu-In solder. Trans China Weld Ins. 2011;32(11):69-72.
[14] Ismail N, Yusoff WYW, Amat A, Manaf NAA, Ahmad N. A review of extreme condition effects on solder joint reliability: understanding failure mechanisms. Def Technol. 2024;41:134-58.
[15] Wang M, Wang J, Ke W. Corrosion behavior of Sn–3.0 Ag–0.5 Cu solder under high-temperature and high-humidity condition. J Mater Sci: Mater Electron. 2014;25:1228-36.
[16] Wang X, Kumagai S, Yoshimura N. Acid rain affecting the electrical properties of outdoor composite dielectric materials. Jpn J Appl Phys. 1998;37:6476.
[17] Jumali N, Mohamad AA, Mohd Nazeri MF. Corrosion properties of Sn-9Zn solder in acidic solution. Mater Sci Forum. 2017;888:365-72.
[18] Nordarina J, Mohd HZ, Ahmad AM, Muhammad FMN. Corrosion behaviour of Sn-based lead-free solders in acidic solution. IOP Conf Ser: Mater Sci Eng. 2018;318:012003.
[19] Nurwahida MZ, Mukridz MM, Ahmad AM, Muhammad FMN. Corrosion properties of SAC305 solder in different solution of HCl and NaCl. IOP Conf Ser: Mater Sci Eng. 2018;318:012004.
[20] Wierzbicka-Miernik A, Guspiel J, Zabdyr L. Corrosion behavior of lead-free SAC-type solder alloys in liquid media. Arch Civ Mech Eng. 2015;15(1):206-13.

[21] ASTM. ASTM G92-17: Standard Test Methods for Vickers Hardness and Knoop Hardness of Metallic Materials. West Conshohocken: ASTM; 2017.
[22] ASTM. ASTM G31-21: Standard Guide for Laboratory Immersion Corrosion Testing of Metals. West Conshohocken: ASTM; 2021.
[23] Lal N, Singh H. The effects of simulated acid rain of different pH-levels on biomass and leaf area in Sunflower (*Helianthus annuus*). Curr Bot. 2012;3(5):45-50.
[24] Lee S. The third periodic report on the state of acid deposition in East Asia, part II national assessments. Japan: Acid deposition monitoring network in East Asia (EANET); 2016.
[25] Lv Y, Yang W, Mao J, Li Y, Zhang X, Zhan Y. Effect of graphene nano-sheets additions on the density, hardness, conductivity, and corrosion behavior of Sn–0.7 Cu solder alloy. J Mater Sci: Mater Electron. 2020;31:202-11.
[26] El-Daly AA, El-Tantawy F, Hammad AE, Gaafar MS, El-Mossalamy EH, Al-Ghamdi AA. Structural and elastic properties of eutectic Sn–Cu lead-free solder alloy containing small amount of Ag and In. J Alloys Compd. 2011;509(26):7238-46.
[27] El-Daly AA, Hammad AE. Enhancement of creep resistance and thermal behavior of eutectic Sn–Cu lead-free solder alloy by Ag and In-additions. Mater Des. 2012;40:292-8.
[28] Tan S, Zou M, Chen B, Zhang Z, Chen W, Hu X, et al. Effects of In and aging treatment on the microstructure, mechanical properties and electrochemical corrosion behavior of Sn–2Cu solder alloy. Mater Charact. 2024;209:113740.
[29] Liu XJ, Liu HS, Ohnuma I, Kainuma R, Ishida K, Itabashi S, et al. Experimental determination and thermodynamic calculation of the phase equilibria in the Cu–In–Sn system. J Electron Mater. 2001;30:1093-103.
[30] Tian S, Li S, Zhou J, Xue F. Thermodynamic characteristics, microstructure and mechanical properties of Sn–0.7Cu–xIn lead-free solder alloy. J Alloys Compd. 2018;742:835-43.
[31] Tian S, Li S, Zhou J, Xue F, Cao R, Wang F. Effect of indium addition on interfacial IMC growth and bending properties of eutectic Sn–0.7Cu solder joints. J Mater Sci: Mater Electron. 2017;28:16120-32.
[32] Khaled KF, Fadl-Allah SA, Hammouti B. Some benzotriazole derivatives as corrosion inhibitors for copper in acidic medium: experimental and quantum chemical molecular dynamics approach. Mater Chem Phys. 2009;117(1):148-55.
[33] Gao YF, Cheng CQ, Zhao J, Wang LH, Li XG. Electrochemical corrosion of Sn–0.75Cu solder joints in NaCl solution. Trans Nonferrous Met Soc China. 2012;22(4):977-82.
[34] Jaffery HA, Sabri MFM, Said SM, Hasan SW, Sajid IH, Nordin NIM, et al. Electrochemical corrosion behavior of Sn–0.7Cu solder alloy with the addition of bismuth and iron. J Alloys Compd. 2019;810:151925.
[35] Jaiswal D, Singh V, Pathote D, Behera CK. Electrochemical behaviour of lead-free Sn–0.7Cu–xIn solders alloys in 3.5 wt% NaCl solution. J Mater Sci: Mater Electron. 2021;32:23371-84.
[36] Jaiswal D, Pathote D, Singh V, Behera CK. Effect of Al addition on electrochemical behavior of Sn–0.7Cu–xAl lead-free solders alloys in 3.5 wt.% NaCl solution. J Mater Eng Perform. 2022;31:7550-60.
[37] Jaiswal D, Pathote D, Singh V, Kumar MR, Behera CK. Effect of Ti addition on the electrochemical behaviour of Sn–0.7Cu–xTi lead-free solders alloys in 3.5 wt.% NaCl solution. Bull Mater Sci. 2024;47:282.
[38] Aziz MZH, Zainon N, Mohamad AA, Nazeri MFM. Corrosion investigation of Sn-0.7Cu Pb-free solder in open-circuit and polarized conditions. IOP Conf Ser: Mater Sci Eng. 2020;957:012012.
[39] Guśpiel J, Wierzbicka-Miernik A, Reczyński W. Kinetics of corrosion process in H2SO4 and HNO3 aqueous solutions of lead free Sn–Ag–Cu solder alloys. Arch Metall Mater. 2016;61(2):559-68.
[40] Huang HZ, Lu D, Shuai GW, Wei XQ. Effects of phosphorus addition on the corrosion resistance of Sn–0.7Cu lead-free solder alloy. Trans Indian Inst Met. 2016;69:1537-43.
[41] Jiao X, Yang Z, Yan J, Zhang J, Chen X, Guan R. Electrodeposition and corrosion behavior of Cu–Sn alloys in 3.5 wt.% NaCl and 0.1 M HNO3 solutions. Metals. 2025;15(4):426.
[42] McCafferty E. Introduction to Corrosion Science. USA: Springer; 2010.
[43] Horváth B, Illés B, Shinohara T, Harsányi G. Copper-oxide whisker growth on tin-copper alloy coatings caused by the corrosion of Cu6Sn5 intermetallics. J Mater Sci. 2013;48:8052-9.
[44] Tsao LC, Chen CW. Corrosion characterization of Cu–Sn intermetallics in 3.5 wt.% NaCl solution. Corros Sci. 2012;63:393-8.
[45] Pourbaix M. Atlas of Electrochemical Equilibria in Aqueous solutions. New York: Pergamon Press; 1966.
[46] Kanlayasiri K, Mongkolwongrojn M, Ariga T. Influence of indium addition on characteristics of Sn–0.3Ag–0.7Cu solder alloy. J Alloys Compd. 2009;485(1-2):225-30.